Materials Research Proceedings 41 (2024) 2154-2163 https://doi.org/10.21741/9781644903131-237

Fatigue life analysis of hot forming dies produced by the L-PBF and WA-DED additive technologies

ALIMOV Artem[1,a*], SVIRIDOV Alexander[1,b] and HÄRTEL Sebastian[1,c]

[1]Chair of Hybrid Manufacturing, Brandenburg University of Technology, Cottbus, Germany

[a]alimov@b-tu.de, [b]sviridov@b-tu.de, [c]haertel@b-tu.de

Keywords: Fatigue, LCF, Additive Manufacturing, Hot Forming Dies, L-PBF, WA-DED, WAAM

Abstract. Additive manufacturing (AM) technologies are widely used for the production of individual complex precise parts and small-scale production. AM has been used in many applications for the manufacturing of sheet metal forming dies. The production of hot bulk forming dies by additive manufacturing technology has not been extensively studied in the literature. Traditional hot working steels exhibit many problems during the AM process, such as crack formation due to complex thermal processing cycles. Maraging/precipitation-hardened (PH) steels may be a good alternative because of their ability to undergo additive manufacturing. One of the main causes of hot forming die failures is thermomechanical fatigue. The fatigue performance of 17-4PH was investigated primarily during high-cycle fatigue (HCF) and low-cycle fatigue (LCF) modes without heat treatment as well as with H1100 heat treatment. The LCF of dies with the heat treatment designation H900, which is most appropriate for die production, has not been intensively investigated. In this work, the mechanical properties and fatigue life of 17-4PH precipitation-hardened steel produced by laser powder bed fusion (L-PBF) and wire arc direct energy deposition (WA-DED) additive technologies were experimentally investigated, and numerical models for high-temperature low cycle fatigue life were developed for 17-4PH steel. Based on the FEM simulation in the commercial program QForm UK, the fatigue life of the produced dies was predicted.

Introduction

Additive manufacturing (AM) technologies represent methods of layer-by-layer production of three-dimensional objects from a CAD model [1]. The main application fields of AM include the aerospace [2], energy [3] and automotive industries [4] as well as biomedicine [5]. Previously reported AMs were used primarily for rapid prototyping, for the production of individual parts or for small batch production [6], but the rapid development of AMs in recent years has extended the application of these materials to the production of casting molds [7] and sheet metal forming dies [8]. The additive manufacturing of hot bulk forging dies has not been covered as extensively in the literature. Huskic et al. [9] and Junker et al. [10] reported the additive manufacturing of forming dies from 1.2709 and 1.2343 tool steels, respectively. Typically, tool steels tend to develop hot cracks in additive manufacturing [11] and require special measures such as preheating the build plate to high temperatures of up to 800°C for defect-free production.

Currently, the most commonly used additive manufacturing methods are powder bed fusion (PBF) and direct energy deposition (DED) methods [12]. The energy source can be an electric arc, laser, plasma or electron beam. Laser Powder Bed Fusion (L-PBF) technology fabricates complex 3D components from powder by layer-by-layer selective laser melting. It offers one of the highest accuracies among AM technologies [13]. The main disadvantage of L-PBF is the limited workspace and relatively low performance. Wire-arc DED (WA-DED) has the highest productivity among the AM methods. Due to the use of an electric arc, WA-DED is believed to

cause high heat loads during processing [14] and a large heat-affected area [15]; therefore, WA-DED can be utilized only limitedly for the die production.

In an earlier work [16] the feasibility of using lightweight hot forming dies produced from 17-4 steel via L-PBF and WA-DED technologies and their operability was demonstrated. However, the fatigue strength of additive manufactured dies made from 17-4 PH steel requires further study because this is one of the main failure causes of hot forging dies [17]. Hot forging dies have a rather short service life due to high thermomechanical loads [18]; therefore, low cycle fatigue (LCF) is the determining criterion. The fatigue performance of 17-4PH was investigated primarily during high-cycle (HCF) [19] and low-cycle (LCF) fatigue modes without heat treatment [20] as well as with H1100 heat treatment [21]. The LCF of dies with the heat treatment designation H900, which is most appropriate for die production, has not been intensively investigated. In this paper, the mechanical and fatigue properties of AM-processed 17-4PH steel after H900 designation heat treatment are experimentally investigated, the coefficients of the Manson–Coffin–Basquin model are determined, and the prediction of cycles to failure is carried out using QForm UK software.

Materials and Methods

Materials. The material used in the L-PBF process was a 17-4PH powder with a 20–45 μm particle size provided by m4p material solutions GmbH, Magdeburg, Germany.

The material used in the WA-DED process was a 1,2 mm diameter wire made of 17-4PH provided by Metal Technology Canterbo GmbH, Meerbusch, Germany. The chemical composition of the material used is presented in *Table 1*.

Table 1. The chemical composition of the 17-4PH steel

Element	Cr	Ni	Cu	Nb	C	Si	Mn	Fe
Nom.	15,0–17,0	3,0–5,0	3,0–5,0	0,15–0,45	<0,07	<1,00	<0,70	Bal.
L-PBF	16,0	4,0	4,0	0,29	0,03	0,60	0,70	
WA-DED	16,37	4,78	3,63	0,23	0,019	0,46	0,64	

Production of the specimens. The WA-DED process was carried out with a Guttroff robotic welding system using a Fronius TPSi 500 welding source. ArC2 (Argon with 2% CO_2) was used as a shielding gas with a flow rate of 15 L/min. AISI 304 stainless steel plates with dimensions of 50x150x10 mm were used as the substrate and were not preheated during the production process. The dwell time after each deposited layer was 30, 60 and 90 s for layers 1, 2 and 3, respectively, and further 200 s for the remaining layers. One sample block was produced at a time, alternating the starting point and welding direction for each layer. The main parameters of the WA-DED process were the same as those for die production [16] and are listed in *Table 2*.

Table 2. The main parameters of the WA-DED process

Wire feed speed, (m/min)	7,0
Stickout, (mm)	15,0
Welding speed, (mm/min)	400,0
Welding power, (W)	3600
Weld seam width, (mm)	7,5
Layer thickness, (mm)	3,2
Weld seam overlap, (mm)	4,2

The L-PBF process was carried out on an EOS M290 with the parameters provided by the machine manufacturer and were the same as those used for die production [16]. The main parameters of the L-PBF process are listed in *Table 3*.

Table 3. The main parameters of the L-PBF process

Exposure speed, (mm/s)	750,0
Hatching distance, (mm)	0,11
Layer thickness, (μm)	40
Laser power, (W)	220

The WA-DED-deposited block (*Fig. 1, a*) was flat milled, and then, Ø10x60 mm cylindrical samples (*Fig. 1, c*) were extracted longitudinally (0°) and transversally (90°) to the deposition direction using electrical discharge machining. In L-PBF production, 32 samples each longitudinally (0°) and transversally (90°) to the deposition direction were produced simultaneously (*Fig. 1, b*).

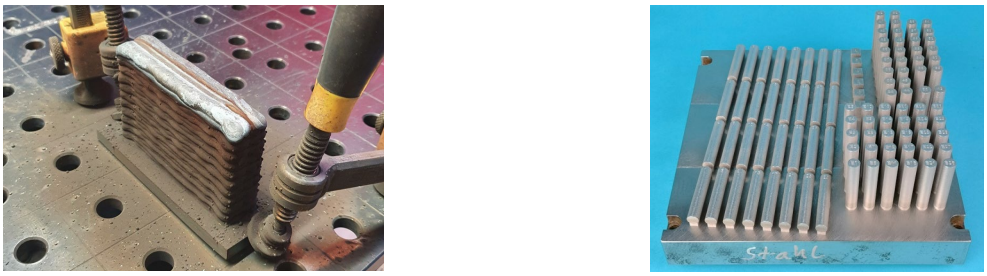

a) b)

Fig. 1. WA-DED-produced block (a), L-PBF-produced cylindrical samples (b)

The samples were heat treated horizontally in a chamber furnace to the H900 designation to maximize the mechanical properties. No visible deformation of the samples was observed during the heat treatment. The heat treatment scheme is shown in *Fig. 2*.

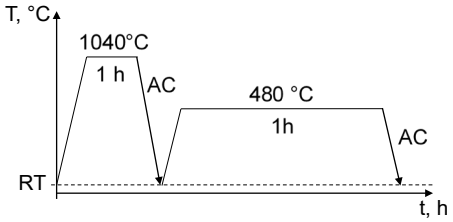

Fig. 2. The heat treatment scheme for 17-4PH steel under the H900 designation

The final stage of specimen fabrication involved turning the specimens according to the final dimensions (*Fig. 3*).

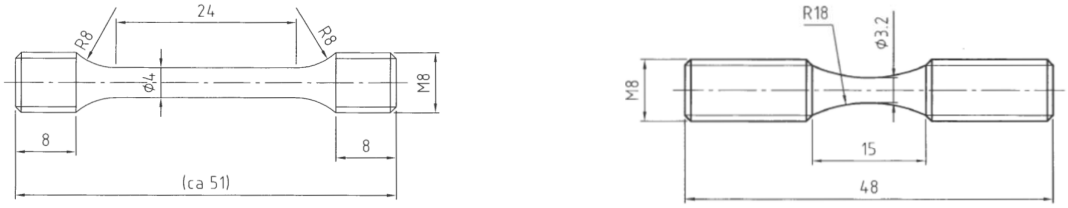

a) b)

Fig. 3. Geometry of the tensile (a) and fatigue (b) test specimens

Microstructural characterization was performed using a Keyence VHX-7000 digital microscope. The microstructure of WA-DED and L-PBF-produced specimens after the heat treatment to the designation H900 is shown in *Fig. 4*.

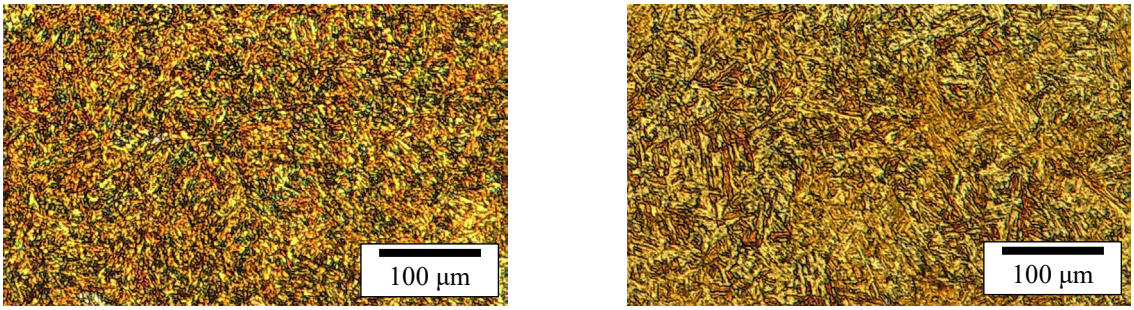

a) b)

Fig. 4. Microstructure of the WA-DED (a) L-PBF-produced (b) specimens

Surface analysis was carried out with a Keyence VK-X1000 3D laser confocal scanning microscope. Surface profile analysis of the specimen gauge length showed that the roughnesses of all the samples after turning were nearly identical and equal to Ra 4.35 ± 0.5.

Test equipment and parameters. Static tensile tests and fatigue tests were carried out with an Instron 8801 ServoHydraulic testing system. The specimen was fixed in M8 threaded holes of adapters made of Waspaloy stainless steel and tightened with AISI 304 steel nuts with a 20 Nm torque. The adapters were clamped in hydraulic grips using notched prismatic wedge inserts. The samples were heated in a three-zone split resistance furnace with automatic temperature control using three thermocouples. The test setup is shown in *Fig. 6*.

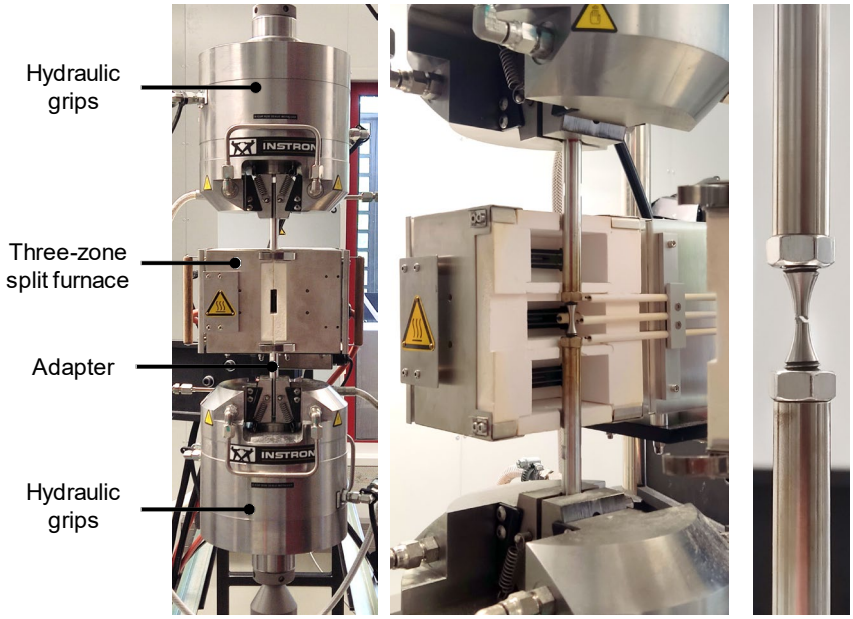

a) b) c)

Fig. 5. Dynamic testing machine Instron 8801 (a), three-zone split furnace (b) and a broken specimen fixed with adapters (c)

The main test parameters are shown in *Table 4.*

Table 4. The main parameters of the tensile and fatigue tests

Test temperature, (°C)	23,2 ± 2,0 200,0 ± 5,0
Static tensile tests	
Test speed, (mm/s)	1,0
Fatigue tests	
Control	σ_a
Frequency, (Hz)	20,0
Cycle asymmetry coefficient R	-1

FEM simulation. Simulations were performed with the commercial FEM software QForm UK 11.0.1 (QForm Group FZ LLC, Fujairah, United Arab Emirates) in a general forming module. The forging process and simulation parameters are described in detail in [16].

Manson-Coffin-Basquin equation with Morrow's mean stress correction [22] implemented in QForm UK [23] was used for the prediction of fatigue life:

$$\frac{\Delta\epsilon}{2} = \frac{\sigma'_f - \sigma_m}{E}\left(2N_f\right)^b + \epsilon'_f\left(2N_f\right)^c \quad (1)$$

Due to the absence of any considerable plastic strains up to the last few cycles before failure, their influence was neglected. Cyclic hardening and softening effects were also not recognized during fatigue testing and thus were not considered. The equation (1) was used in the following form:

$$\frac{\Delta\sigma}{2} = (\sigma'_f - \sigma_m)\left(2N_f\right)^b \quad (2)$$

A special module for cyclic tool heating was used to obtain an equilibrium temperature during the batch forging process.

The section cuts of the geometry models used in the forging simulation with WA-DED (b) and L-PBF (b) dies are shown in ***Fig. 7***.

a) b)

Fig. 6. The section cuts of the geometry models used in the forging simulation with WA-DED (b) and L-PBF (b) die

Results and discussion

Analysis of die thermomechanical loads. To evaluate fatigue life, it is necessary to determine the temperature and loads to which the hot forging die is subjected. During the continuous forging process, the die does not cool to the initial temperature; therefore, the QForm tool cycling module was used to analyse the steady-state die temperature. The temperature distribution over the die impressions at the end of the forging is shown in *Fig. 8*.

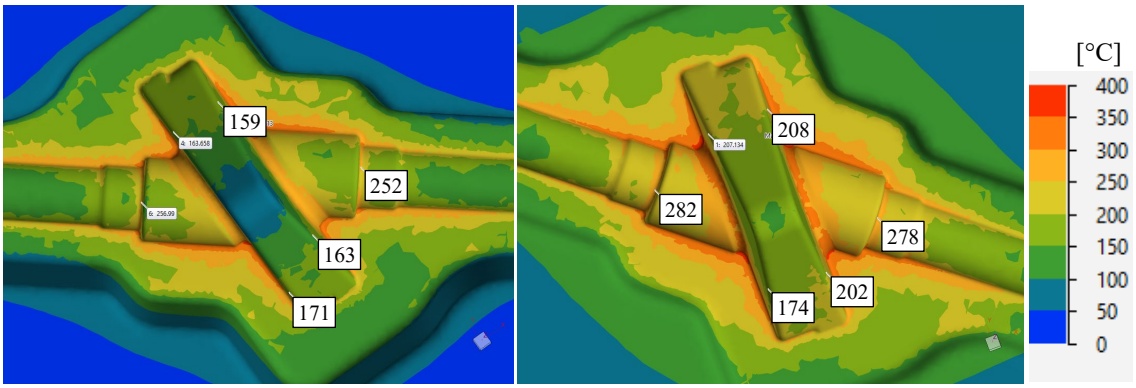

a) b)

Fig. 7. The surface temperature distributions of the WA-DED (a) and L-PBF (b) produced dies

Due to the different designs of the WA-DED and L-PBF dies, the temperature is slightly different and amounts to an average of 200°C. This temperature will be used to analyze mechanical and fatigue properties of WA-DED and L-PBF produced specimens.

The maximum effective stresses occur at the bottom point of the ram stroke at the final moment of forging and are shown in *Fig. 9*. The effective stress in the WA-DED die is approximately 950 MPa, and that in the L-PBF die is approximately 1100 MPa.

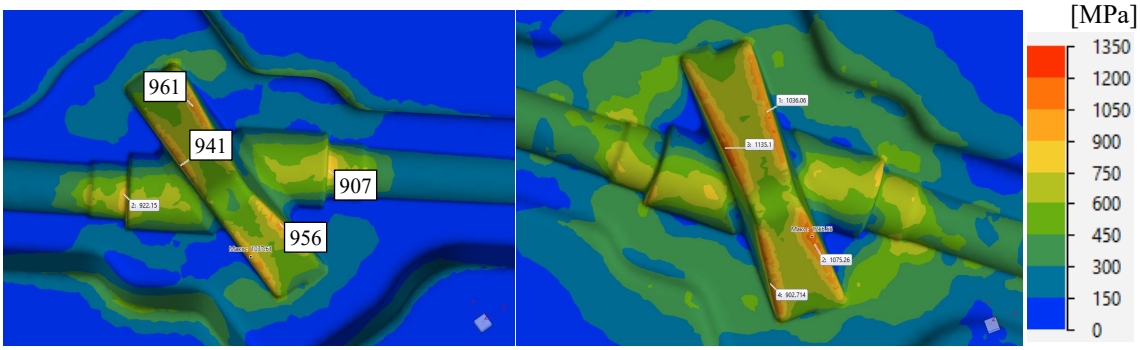

a) b)

Fig. 8. The effective stress surface distribution during forging with WA-DED (a) and L-PBF produced dies

Analysis of the first principal stress distribution (*Fig. 10*) shows that these stresses are mostly tensile. Thus, the corners of the impression cavities are the critical areas.

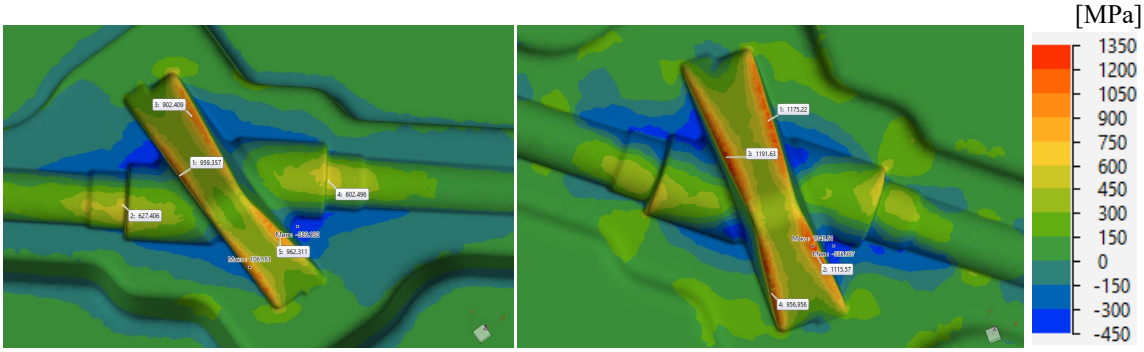

a) b)

Fig. 9. 1st principal stress surface distribution during forging with WA-DED (a) and L-PBF produced dies

A preliminary estimation of the tool fatigue life was carried out with H11 steel as the die material, the parameters of which were set according to the work of Velay et al. [24]. The number of cycles to failure predicted using H11 tool steel shown in *Fig. 11* and equals approximately 400000 and 100000 for WA-DED and L-PBF dies respectively. Due to the lower effective stresses in the WA-DED die, the predicted number of cycles to failure is significantly higher than that of the L-PBF die. However, this prediction does not take into account the fatigue properties of AM-produced materials, which will be investigated further.

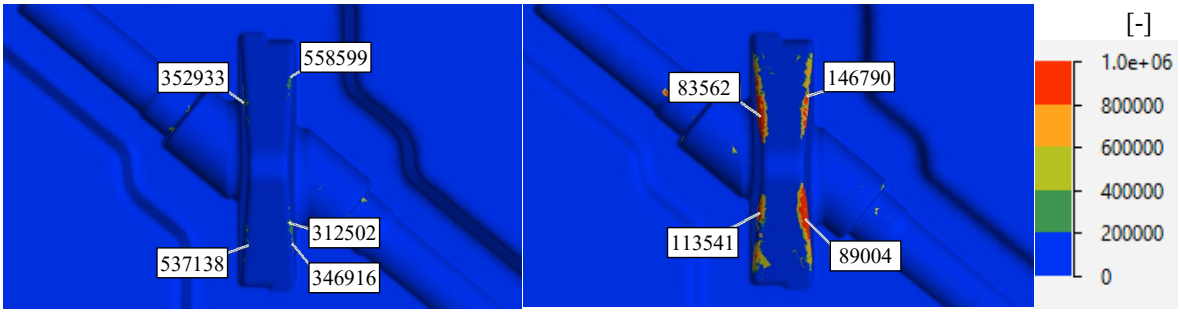

Fig. 10. Cycles to failure using H11 tool steel for WA-DED (a) and L-PBF (b) produced dies

Tensile and fatigue testing. Flow curves at RT and 200°C for the WA-DED- and L-PBF-produced specimens after the H900 heat treatment are shown in *Fig. 12*.

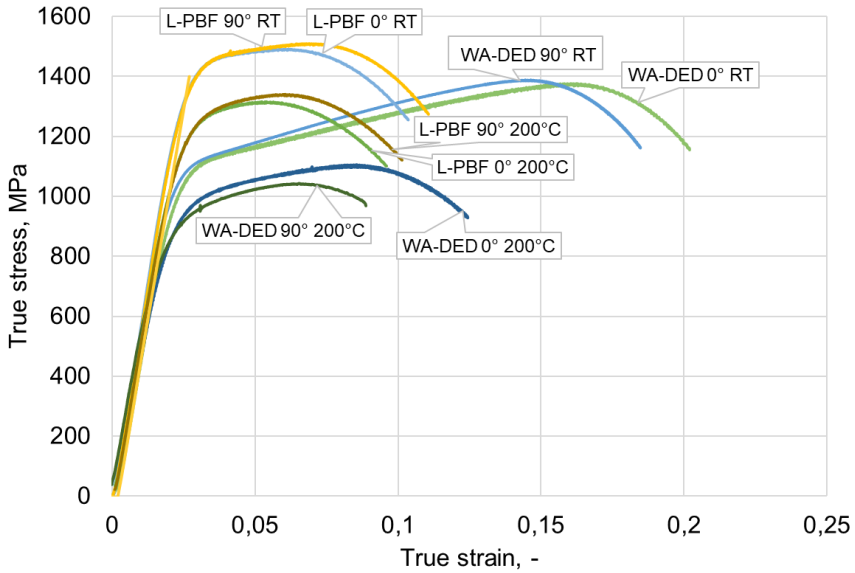

Fig. 11. Flow curves at RT and 200°C for the WA-DED- and L-PBF-produced specimens

Compared with the specimens made by L-PBF, the specimens made by WA-DED exhibit significantly lower ultimate tensile strength at room temperature, but they still fulfil the H900 destination requirements. The yield strength of the WA-DED made specimens no longer met the requirements of the H900 designation. At 200°C, neither the ultimate tensile strength nor yield strength of the samples made by WA-DED meet the requirements of the H900 designation. The specimens made by L-PBF meet the requirements of the standard H900 heat treatment conditions both at room temperature and at 200°C. The mechanical property comparison results of the WA-DED- and L-PBF-fabricated specimens are shown in *Fig. 13*.

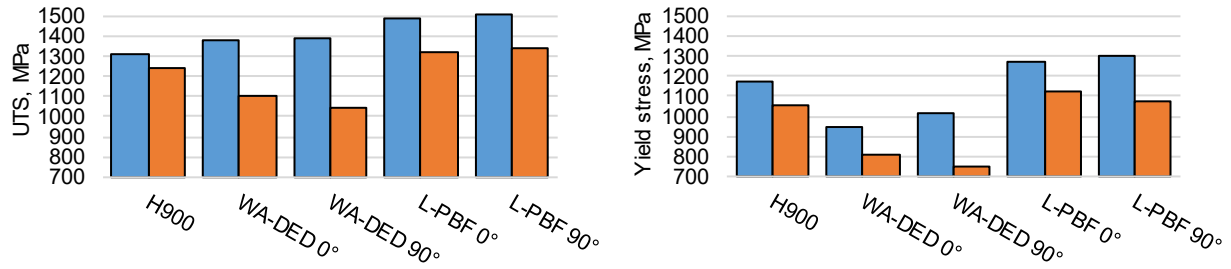

a) b)

Fig. 12. Comparison of the ultimate tensile strength (a) and yield stress (b) at RT (blue columns) and 200°C (orange columns) for the WA-DED- and L-PBF-produced specimens

At both room temperature and 200°C, the L-PBF specimens exhibited significantly higher fatigue properties than did the WA-DED specimens. Wöhler diagrams of the WA-DED and L-PBF produced specimens are shown in ***Fig. 14***.

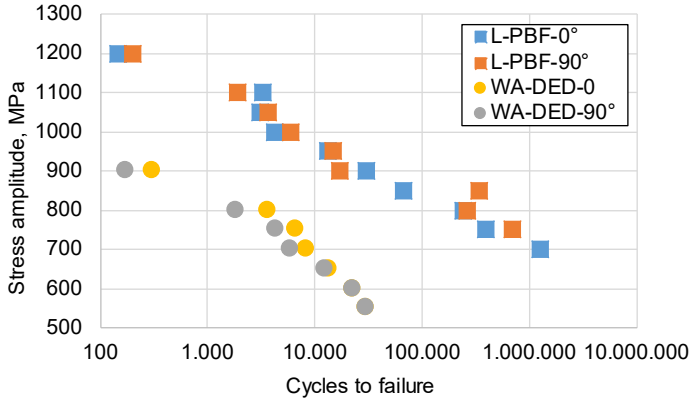

Fig. 13. Wöhler diagrams of the WA-DED- and L-PBF-produced specimens

Die fatigue life analysis. The parameters of the tool fatigue life model were determined using the least squares method and are presented in *Table 3*.

Table 5. The parameters of the tool fatigue life model

Parameter	WA-DED	L-PBF
$\sigma'_f, (MPa)$	1628,191	1739,161
b	−0,09	−0,059

Fatigue analysis (*Fig. 15*) showed that the die made by WA-DED has a significantly lower fatigue strength than the die made by L-PBF. The number of cycles to failure of the WA-DED die is approximately 10000, whereby the predicted failure area includes all cavities as well as an edge on the workpiece bar where no fatigue failure was initially predicted. The L-PBF-fabricated die exhibited significantly higher fatigue strength than the WA-DED- produced die, with the area of predicted fatigue failure being localized at the expected location in the die impression cavity. The predicted number of cycles to failure for the WA-DED die is approximately 6000. Despite the higher effective stresses (*Fig. 9*) due to the lightweight construction of L-PBF dies, the lifetime is significantly longer and amounts to approximately 50000 cycles to failure. This can be explained by higher process-related material properties of L-PBF specimens, which are considerably higher those of WA-DED material even after the H900 heat treatment, what has been proven by static tensile tests as well as fatigue tests.

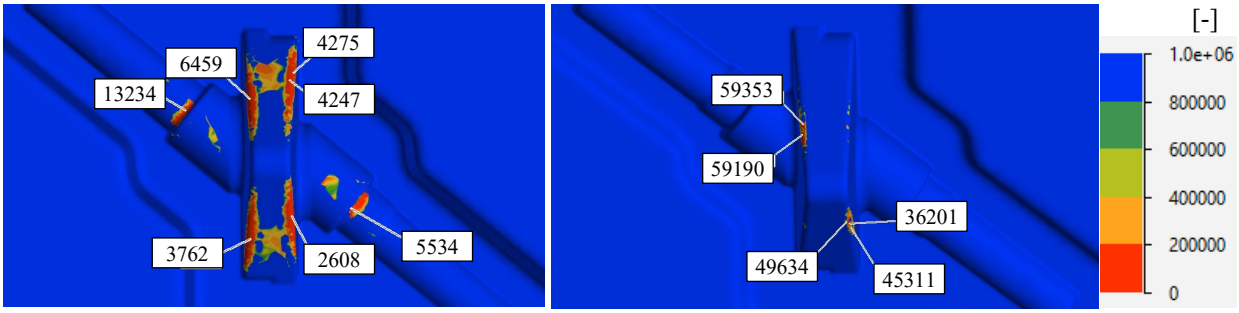

a) b)

Fig. 14. Predicted cycles to failure of the WA-DED (a) and L-PBF (b) produced dies

Conclusions

1. 17-4PH steel is suitable for the production of hot forming dies by AM technologies.
2. L-PBF-produced tools exhibited higher mechanical and fatigue properties than WA-DED-produced tools.
3. Even the resource-efficient production of L-PBF lightweight forming dies with 56% less weight (compared to WA-DED solid dies) leads to a significantly longer lifetime.
4. A numerical model for 17-4PH fatigue life of WA-DED and L-PBF-produced forming dies was developed and implemented in QForm UK software.
5. The fatigue life of AM-produced dies has been predicted and evaluated for small batch hot forging.

References

[1] I. Gibson, D. Rosen, B. Stucker, and M. Khorasani, *Additive Manufacturing Technologies*. Cham: Springer International Publishing, 2021. https://doi.org/10.1007/978-3-030-56127-7

[2] A. Gisario, M. Kazarian, F. Martina, and M. Mehrpouya, "Metal additive manufacturing in the commercial aviation industry: A review," *Journal of Manufacturing Systems*, 53 (2019) 124–149. https://doi.org/10.1016/j.jmsy.2019.08.005

[3] C. Sun, Y. Wang, M. D. McMurtrey, N. D. Jerred, F. Liou, and J. Li, "Additive manufacturing for energy: A review," *Applied Energy*, 282 (2021) 116041. https://doi.org/10.1016/j.apenergy.2020.116041

[4] S. G. Scholz, R. J. Howlett, and R. Setchi, Eds., *Sustainable Design and Manufacturing: Proceedings of the 8th International Conference on Sustainable Design and Manufacturing (KES-SDM 2021)*, in Smart Innovation, Systems and Technologies, vol. 262. Singapore: Springer Singapore, 2022. https://doi.org/10.1007/978-981-16-6128-0

[5] A. J. Sheoran, H. Kumar, P. K. Arora, and G. Moona, "Bio-Medical applications of Additive Manufacturing: A Review," *Procedia Manufacturing*, 51 (2020) 663–670. https://doi.org/10.1016/j.promfg.2020.10.093

[6] G. Liu *et al.*, "Additive manufacturing of structural materials," *Materials Science and Engineering: R: Reports*, 145 (2021) 100596. https://doi.org/10.1016/j.mser.2020.100596

[7] M. Gao, L. Li, Q. Wang, Z. Ma, X. Li, and Z. Liu, "Integration of Additive Manufacturing in Casting: Advances, Challenges, and Prospects," *Int. J. of Precis. Eng. and Manuf.-Green Tech.*, 9 (2022) 305–322. https://doi.org/10.1007/s40684-021-00323-w

[8] D. Chantzis *et al.*, "Review on additive manufacturing of tooling for hot stamping," *Int J Adv Manuf Technol*, 109 (2020) 87-107. https://doi.org/10.1007/s00170-020-05622-1

[9] A. Huskic, B. Behrens, J. Giedenbacher, and A. Huskic, "Standzeituntersuchungen generativ hergestellter Schmiedewerkzeuge," *Schmiede J*, 92013 2013) 66–70.

[10] D. Junker, O. Hentschel, R. Schramme, M. Schmidt, and M. Merklein, "Performance of hot forging tools built by laser metal deposition of hot work tool steel X37CrMoV5-1," in *Proceedings of the laser in manufacturing conference*, 2017.

[11] R. Stache, "Untersuchungen zur Herstellung von Werkzeugelementen für das Presshärten mittels Laser Beam Melting," PhD, Technische Universität Chemnitz, Chemnitz, 2020.

[12] "DIN EN ISO/ASTM 52900:2022-03 Additive Fertigung - Grundlagen – Terminologie."

[13] S. L. Sing and W. Y. Yeong, "Laser powder bed fusion for metal additive manufacturing: perspectives on recent developments," *Virtual and Physical Prototyping*, 15 (2020) 359–370. https://doi.org/10.1080/17452759.2020.1779999

[14] Ayed, A. et al. (2020). Effects of WAAM Process Parameters on Metallurgical and Mechanical Properties of Ti-6Al-4V Deposits. In: Chaari, F., et al. Advances in Materials, Mechanics and Manufacturing. Lecture Notes in Mechanical Engineering. Springer, Cham. https://doi.org/10.1007/978-3-030-24247-3_4

[15] M. Benakis, D. Costanzo, and A. Patran, "Current mode effects on weld bead geometry and heat affected zone in pulsed wire arc additive manufacturing of Ti-6-4 and Inconel 718," *Journal of Manufacturing Processes*, 60 (2020) 61–74. https://doi.org/10.1016/j.jmapro.2020.10.018

[16] A. Alimov, A. Sviridov, B. Sydow, F. Jensch, and S. Härtel, "Additive manufacturing of hot-forming dies using laser powder bed fusion and wire arc direct energy deposition technologies," *Metals*, 13 (2023) 1842. https://doi.org/10.3390/met13111842

[17] A. A. Emamverdian, Y. Sun, C. Cao, C. Pruncu, and Y. Wang, "Current failure mechanisms and treatment methods of hot forging tools (dies) - a review," *Engineering Failure Analysis*, vol. 129 (2021) 105678. https://doi.org/10.1016/j.engfailanal.2021.105678

[18] Z. Gronostajski, M. Kaszuba, S. Polak, M. Zwierzchowski, A. Niechajowicz, and M. Hawryluk, "The failure mechanisms of hot forging dies," *Materials Science and Engineering: A*, 657 (2016) 147–160. https://doi.org/10.1016/j.msea.2016.01.030

[19] J. Radhakrishnan, P. Kumar, S. S. Gan, A. Bryl, J. McKinnell, and U. Ramamurty, "Fatigue resistance of the binder jet printed 17-4 precipitation hardened martensitic stainless steel," *Materials Science and Engineering: A*, 865 (2023) 144451. https://doi.org/10.1016/j.msea.2022.144451

[20] F. Concli, L. Fraccaroli, F. Nalli, and L. Cortese, "High and low-cycle-fatigue properties of 17–4 PH manufactured via selective laser melting in as-built, machined and hipped conditions," *Prog Addit Manuf*, 7 (2022) 99–109. https://doi.org/10.1007/s40964-021-00217-y

[21] L. Carneiro, B. Jalalahmadi, A. Ashtekar, and Y. Jiang, "Cyclic deformation and fatigue behavior of additively manufactured 17–4 PH stainless steel," *International Journal of Fatigue*, 123 (2019) 22–30. https://doi.org/10.1016/j.ijfatigue.2019.02.006

[22] S. Suresh, *Fatigue of materials*, Cambridge University Press, 1998. https://doi.org/10.1017/CBO9780511806575

[23] A. V. Vlasov, "Thermomechanical fatigue of dies for hot stamping," *Steel Transl.*, 46 (2016) 356–360. https://doi.org/10.3103/S0967091216050156

[24] V. Velay, G. Bernhart, D. Delagnes, and L. Penazzi, "A continuum damage model applied to high-temperature fatigue lifetime prediction of a martensitic tool steel," *Fatigue Fract Eng Mat Struct*, 28 (2005) 1009–1023. https://doi.org/10.1111/j.1460-2695.2005.00939.x